Journal of Engineering Sciences, Assiut University, Vol. 35, No. 3 pp. 729-742, May 2007

VISUALIZATION OF THE EFFECT OF UPFC ON POWER FLOW CHARACTERESTICS

A. Ahmed
Electrical Engineering Department, Faculty of Engineering, Assiut University, Assiut, Egypt E-mail: a_ahmed@aun.edu.eg

(Received March 27, 2007 Accepted, April 3, 2007)

This paper presents an investigation and visualization of the effect of UPFC on power flow characteristics by incorporating it in a simple two-bus system. The UPFC is represented by two ideal voltage sources each of them is connected in series with a reactance. This model investigates the nonlinearity of UPFC on the power system load flow problem. Since the various UPFC variables equations are non-linear, a form of vector presentation in complex power plane is used to visualize the effect of different control variables of UPFC on line power transfer. This visualization helps to identify the effectiveness of each one of control variables on power control region.

KEYWORDS: *Flexible AC transmission systems (FACTS), Unified power flow controller (UPFC), Load flow analysis, MATLAB.*

1. INTRODUCTION

The Unified Power Flow Controller (UPFC) was proposed [1] for real-time control and dynamic compensation of AC transmission systems, providing the necessary functional flexibility required to solve many of the problems facing the utility industry. The UPFC consists of two switching converters, which in the implementations considered are voltage-sourced inverters using gate turn-off (GTO) thyristor valves, as illustrated in Fig. 1 [1-2]. These inverters, labeled "Inverter 1" and "Inverter 2" in the figure, are operated from a common DC link provided by a DC storage capacitor. This arrangement functions as an ideal AC-to-AC power converter in which the real power can freely flow in either direction between the two terminals of the two inverters and each inverter can independently generate (or absorb) reactive power at its own AC output terminal. Inverter 2 provides the main function of the UPFC by injecting an AC voltage V_{ser} with controllable magnitude ($0 \le V_{ser} \le V_{ser\,max}$) and phase angle $\theta_{ser}(0 \le \theta_{ser} \le 360^{\circ})$, at the power frequency, in series with line via an insertion transformer. This injected voltage can be considered essentially as a synchronous voltage source [2-5]. The transmission line current flows through this voltage source resulting in real and reactive power exchange between it and the AC system. The real power exchanged at the AC terminal is converted by the inverter into DC power, which appears at the DC link as positive or negative real power demand. The reactive power exchanged at the AC terminal is generated internally by the inverter.

The basic function of inverter 1 is to supply or absorb the real power demanded by inverter 2 at the common DC link. This DC link power is converted back to AC and coupled to the transmission line via a shunt-connected transformer.

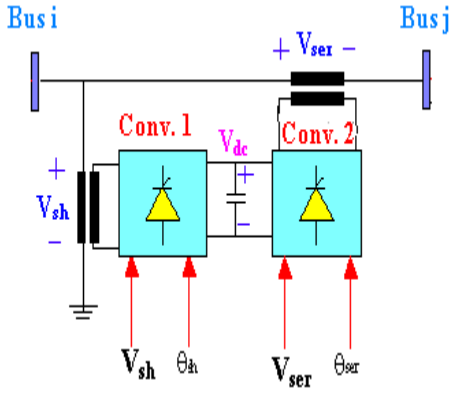

Fig. (1): UPFC basic structure.

Inverter 1 can also generate or absorb controllable reactive power, if it is desired, and thereby it can provide independent shunt reactive compensation for the line. It is important to note that whereas there is a closed "direct" path for the real power negotiated by the action of series voltage injection through inverters 1 and 2 back to the line, the corresponding reactive power exchanged is supplied or absorbed locally by inverter 2 and therefore it does not flow through the line. Thus, inverter 1 can be operated at a unity power factor or be controlled to have a reactive power exchange with the line independently of the reactive power exchanged by inverter 2. This means that there is no continuous reactive power flow through the UPFC.

2. STEADY-STATE CHARACTERISTICS OF UPFC

A power transmission system composed of a line equipped with UPFC can adequately demonstrate basic characteristics of the UPFC for steady-state conditions. Fig. (2) shows a single-phase equivalent circuit of such a system [6-7]. The line is connected between two voltage buses $V_1\angle\delta_1$ and $V_2\angle\delta_2$. The UPFC is represented by an ideal series voltage and shunt voltage source each connected with a series reactance. Series reactance of voltage source $V_{ser}\angle\theta_{ser}$ is included in X_2. The UPFC controls power flow of the line through continuous control of V_{ser} and θ_{ser}. Depending upon the system operating conditions, voltage source $V_{ser}\angle\theta_{ser}$ exchanges real and reactive power with the system. Since a UPFC can neither absorb nor deliver real power (losses are neglected), phase angle θ_{sh} is adjusted to compensate for real power exchange between $V_{sh}\angle\theta_{sh}$ and the system. V_{sh} can be adjusted to compensate for the reactive power exchange between $V_{ser}\angle\theta_{ser}$ and the system. In general, by means of controlling V_{sh}, the net reactive power exchange between the UPFC and the system can be regulated [7].

In order to visualize the effect of the UPFC control variables, (V_{ser}, θ_{ser}, V_{sh}, and θ_{sh}), on the power flow characteristics, it is required to obtain expressions for sending-end and receiving-end powers as a function of these control variables, this can be achieved as follow:

Applying KCL and KVL to the system of Fig. (2), to obtain the system current components.

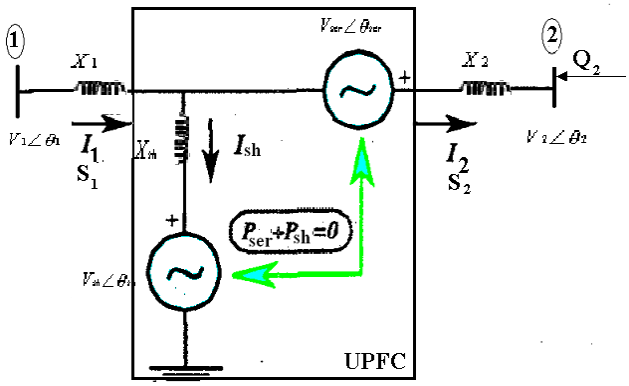

Fig. (2): Single-line diagram of transmission line and UPFC

$$I_1 = I_2 + I_{sh} \quad (1)$$

$$V_1\angle\delta_1 = jX_1I_1 + jX_{sh}I_{sh} + V_{sh}\angle\theta_{sh} \quad (2)$$

$$V_2\angle\delta_2 + V_{ser}\angle\theta_{ser} = jX_2I_2 + jX_{sh}I_{sh} + V_{sh}\angle\theta_{sh} \quad (3)$$

By substitution of I_{sh} from equation (1) into equations (2) and (3), it is possible to get two equations in two unknowns, I_1, I_2 as equation (4) illustrate.

$$j\begin{bmatrix} X_1 + X_{sh} & -X_{sh} \\ X_{sh} & -(X_2 + X_{sh}) \end{bmatrix}\begin{bmatrix} I_1 \\ I_2 \end{bmatrix} = \begin{bmatrix} V_1\angle\delta_1 - V_{sh}\angle\theta_{sh} \\ V_2\angle\delta_2 - V_{ser}\angle\theta_{ser} - V_{sh}\angle\theta_{sh} \end{bmatrix} \quad (4)$$

Solving the above linear algebraic equation, (4), it is possible to obtain I_1 and I_2.

$$I_1 = \frac{1}{X_t^2\angle 90}\begin{bmatrix} (X_{sh} + X_2)V_1\angle\delta_1 - X_2V_{sh}\angle\theta_{sh} \\ + X_{sh}V_{ser}\angle\theta_{ser} - X_{sh}V_2\angle\delta_2 \end{bmatrix} \quad (5)$$

$$I_2 = \frac{1}{X_t^2\angle 90}\begin{bmatrix} X_{sh}V_1\angle\delta_1 + X_1V_{sh}\angle\theta_{sh} \\ +(X_{sh} + X_1)V_{ser}\angle\theta_{ser} - (X_{sh} + X_1)V_2\angle\delta_2 \end{bmatrix} \quad (6)$$

From equations (5) and (6) it is possible to obtain I_{sh} by substitution in equation (1)

$$I_{sh} = \frac{1}{X_t^2\angle 90}\begin{bmatrix} X_2V_1\angle\delta_1 - (X_1 + X_2)V_{sh}\angle\theta_{sh} \\ -X_1V_{ser}\angle\theta_{ser} + X_1V_2\angle\delta_2 \end{bmatrix} \quad (7)$$

Where $X_t = X_1X_2 + X_1X_{sh} + X_2X_{sh}$.

After obtaining the system current components and UPFC shunt current, it is possible to get expressions for the sending-end, receiving-end and UPFC powers as follow:

The sending-end power S_1 can be expressed as:

$$S_1 = P_1 + jQ_1 = V_1 I_1^* = \frac{(X_{sh} + X_2)V_1^2}{X_t^2} \angle 90 - \frac{X_{sh} V_1 V_2}{X_t^2} \angle(90 + \delta_1 - \delta_2) - \frac{X_2 V_1 V_{sh}}{X_t^2} \angle(90 + \delta_1 - \theta_{sh}) + \frac{X_{sh} V_1 V_{ser}}{X_t^2} \angle(90 + \delta_1 - \theta_{ser}) \quad (8)$$

$$P_1 = \frac{X_{sh} V_1 V_2}{X_t^2} \sin(\delta_1 - \delta_2) + \frac{X_2 V_1 V_{sh}}{X_t^2} \sin(\delta_1 - \theta_{sh}) - \frac{X_{sh} V_1 V_{ser}}{X_t^2} \sin(\delta_1 - \theta_{ser}) \quad (9)$$

$$Q_1 = \frac{(X_{sh} + X_2)V_1^2}{X_t^2} - \frac{X_{sh} V_1 V_2}{X_t^2} \cos(\delta_1 - \delta_2) - \frac{X_2 V_1 V_{sh}}{X_t^2} \cos(\delta_1 - \theta_{sh}) + \frac{X_{sh} V_1 V_{ser}}{X_t^2} \cos(\delta_1 - \theta_{ser}) \quad (10)$$

The receiving-end power can be expressed as:

$$S_2 = P_2 - jQ_2 = V_2 I_2^* = -\frac{(X_{sh} + X_1)V_2^2}{X_t^2} \angle 90 + \frac{X_{sh} V_1 V_2}{X_t^2} \angle(90 + \delta_2 - \delta_1) + \frac{X_1 V_2 V_{sh}}{X_t^2} \angle(90 + \delta_2 - \theta_{sh}) + \frac{(X_{sh} + X_1)V_2 V_{ser}}{X_t^2} \angle(90 + \delta_2 - \theta_{ser}) \quad (11)$$

$$P_2 = \frac{X_{sh} V_1 V_2}{X_t^2} \sin(\delta_1 - \delta_2) - \frac{X_1 V_2 V_{sh}}{X_t^2} \sin(\delta_2 - \theta_{sh}) - \frac{(X_{sh} + X_1)V_2 V_{ser}}{X_t^2} \sin(\delta_2 - \theta_{ser}) \quad (12)$$

$$Q_2 = \frac{(X_{sh} + X_1)V_2^2}{X_t^2} - \frac{X_{sh} V_1 V_2}{X_t^2} \cos(\delta_2 - \delta_1) - \frac{X_1 V_2 V_{sh}}{X_t^2} \cos(\delta_2 - \theta_{sh}) - \frac{(X_{sh} + X_1)V_2 V_{ser}}{X_t^2} \cos(\delta_2 - \theta_{ser}) \quad (13)$$

The UPFC series converter power can be expressed as:

$$P_{ser} = -\frac{X_{sh}V_{ser}V_1}{X_t^2}\sin(\theta_{ser}-\delta_1) - \frac{X_1V_{ser}V_{sh}}{X_t^2}\sin(\theta_{ser}-\theta_{sh}) + \frac{(X_{sh}+X_1)V_2V_{ser}}{X_t^2}\sin(\theta_{ser}-\delta_2) \quad (14)$$

$$Q_{ser} = \frac{(X_{sh}+X_1)V_{ser}^2}{X_t^2} + \frac{X_{sh}V_{ser}V_1}{X_t^2}\cos(\theta_{ser}-\delta_1) + \frac{X_1V_{ser}V_{sh}}{X_t^2}\cos(\theta_{ser}-\theta_{sh}) - \frac{(X_{sh}+X_1)V_2V_{ser}}{X_t^2}\cos(\theta_{ser}-\delta_2) \quad (15)$$

The UPFC shunt converter power can be expressed as:

$$P_{sh} = \frac{X_2V_{sh}V_1}{X_t^2}\sin(\theta_{sh}-\delta_1) + \frac{X_1V_{ser}V_{sh}}{X_t^2}\sin(\theta_{sh}-\theta_{ser}) - \frac{X_1V_2V_{sh}}{X_t^2}\sin(\theta_{sh}-\delta_2) \quad (16)$$

$$Q_{sh} = \frac{(X_2+X_1)V_{sh}^2}{X_t^2} - \frac{X_2V_{sh}V_1}{X_t^2}\cos(\theta_{sh}-\delta_1) + \frac{X_1V_{ser}V_{sh}}{X_t^2}\cos(\theta_{sh}-\theta_{ser}) - \frac{X_1V_2V_{sh}}{X_t^2}\cos(\theta_{sh}-\delta_2) \quad (17)$$

From (8) to (17) it is obvious that the equation sets of UPFC are highly non-linear and the effect of every control variable on power flow is not clear. To set the control variables and find the borders of limitations of these variables a visualized presentation of the UPFC control variables is very helpful.

Neglecting UPFC losses, during steady-state operation, the UPFC neither absorbs real power from the system nor injects real power in the system ($P_{ser} + P_{sh} = 0$). Physical interpretation of this statement is that the voltage dc link capacitor remains constant at its pre-specified value V_{dc}. This constraint must be satisfied by the UPFC steady state equations.

The constraint $P_{ser} + P_{sh} = 0$ implies that:

1-No real power is exchanged between the UPFC and the system; thus, the dc link voltage remains constant.

2-The two voltage sources V_{ser} and V_{sh} are mutually dependant.

Assuming that variable θ_{sh} is assigned to regulate the dc link voltage, power flow (both real and reactive) can be simultaneously controlled/changed by variables θ_{ser}, V_{ser} and V_{sh} of the UPFC. Among θ_{ser}, V_{ser} and V_{sh}, the control variable of θ_{ser} has the most dominant effect on the magnitude of real power flow.

According to the above assumptions it is possible to visualize the effect of UPFC control variables on the power flow through the transmission line.

3. EFFECTS OF $V_{ser}\angle\theta_{ser}$ ON SENDING-END, RECEIVING-END AND UPFC POWERS AT CERTAIN TRANSMISSION ANGLE δ AND SHUNT VOLTAGE SOURCE MAGNITUDE V_{SH}.

Figs. (3a through 3d) and Figs. (4a through 4d) show the real and reactive power of the sending-end, receiving-end, UPFC series converter and UPFC shunt converter respectively, versus θ_{ser} that changed from 0° to 360° at different values of V_{ser} from 0 to 0.15 p.u, transmission angle $\delta = 25^{\circ}$, $X_1 = X_2 = 0.5$ p.u and $V_{sh} = 0.9$ p.u. Figs. (3a) and (3b) show that the sending-end and receiving-end real powers are equals according to the constraint of $P_{ser} + P_{sh} = 0$. This constraint shown in Figs. (3c) and (3d), where $P_{ser} = -P_{sh}$. Figures (4a) and (4b) show that the sending-end and receiving-end reactive powers are equals at $V_{ser} = 0$, where in this case $Q_{ser} = 0$ as shown in Fig. (4c). Figure (4d) shows that UPFC absorb shunt reactive power from the system where V_{sh} in this case is less than the system voltage. As V_{ser} increase, the reactive power in all sides will be changed with the change of θ_{ser} in the form of sine wave as illustrated in the previous equations and shown in Figs. (4a) through (4d).

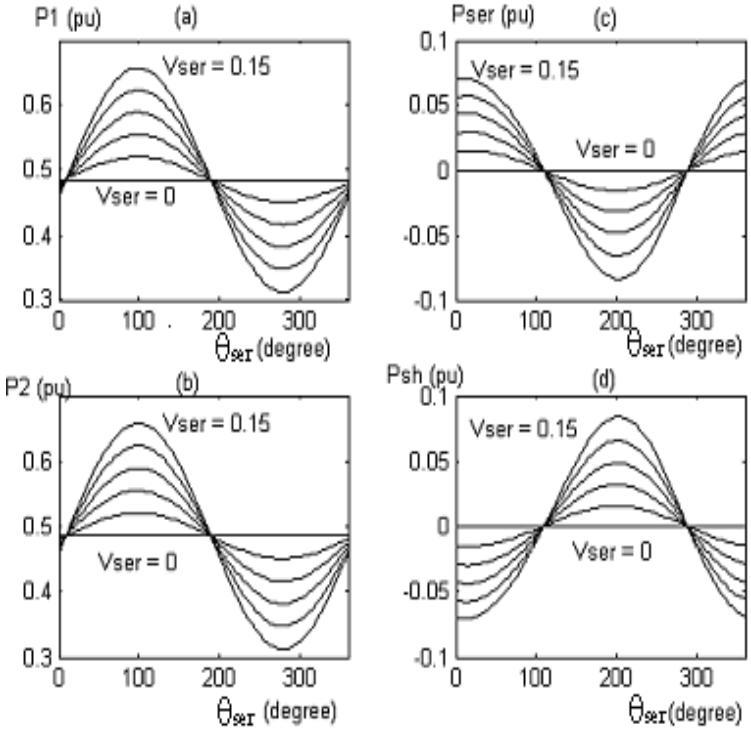

Fig. (3): (a) Sending-end, (b) Receiving-end, (c) Series converter, and (d), Shunt converter, real powers versus θ_{ser} at different values of V_{ser} (0-0.15) p.u.

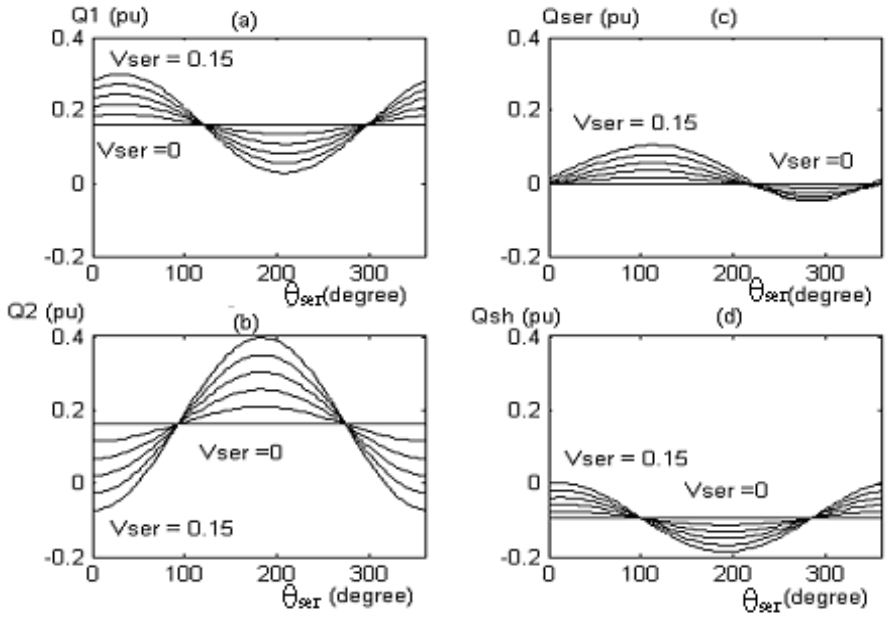

Fig. (4): (a) Sending-end, (b) Receiving-end, (c) Series converter, and (d), Shunt converter, reactive powers versus θ_{ser} at different values of V_{ser} (0-0.15) p.u.

3.1 Power Flow Characteristics at Sending-End

When the UPFC is in service, the complex power at the sending-end of the system of Fig. (2) is given by equation (8) that can be decomposed into four components as given by (18).

$$S_1 = S_a + S_b + S_c + S_d \tag{18}$$

Where S_a to S_d are:

$$\begin{aligned} S_a &= \frac{(X_{sh} + X_2)V_1^2}{X_t^2} \angle 90 \\ S_b &= -\frac{X_{sh}V_1V_2}{X_t^2} \angle 90 + \delta \\ S_c &= -\frac{X_2V_1V_{sh}}{X_t^2} \angle 90 + \delta - \theta_{sh} \\ S_d &= \frac{X_{sh}V_1V_{ser}}{X_t^2} \angle 90 + \delta - \theta_{ser} \end{aligned} \tag{19}$$

Noting that, δ in (19) is equal to δ_1 and the voltage angle of the receiving-end (δ_2) is chosen as the reference angle. Figure (5) graphically represents S_1 in terms of its four components.

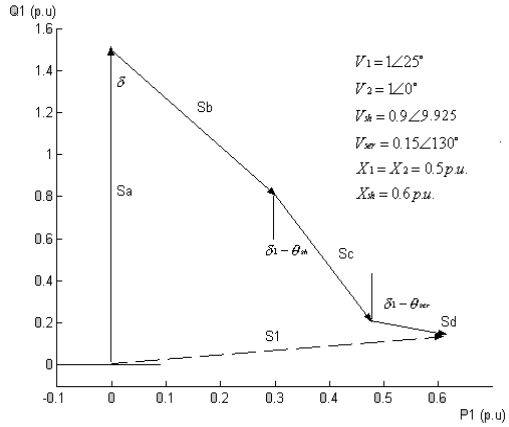

Fig. (5): Graphical representation of S_1 in the complex power plane.

To visualize the effect of UPFC parameters on tie line power flow, it is possible to rewrite (8) as follows:

$$S_1 = A + BV_{sh}\angle -\theta_{sh} + CV_{ser}\angle -\theta_{ser} \qquad (20)$$

Where,

$$A = S_a + S_b \ , \ B = -\frac{X_2 V_1}{X_t^{\,2}}\angle 90 + \delta \ , \text{ and}$$
$$C = \frac{X_{sh} V_1}{X_t^{\,2}}\angle 90 + \delta \qquad (21)$$

In this form, the tie line power is expressed by UPFC control variables ($V_{ser}, \theta_{ser}, V_{sh}, \text{and } \theta_{sh}$). If system parameters are kept unchanged, A,B and C remain constant. Therefore the tie line power flow becomes only as a function of UPFC control variables.

Now we can visualize the effect of the UPFC control variables on power flow characteristics at sending-end. Figure (6) represents Fig. (5) in the form of (20).

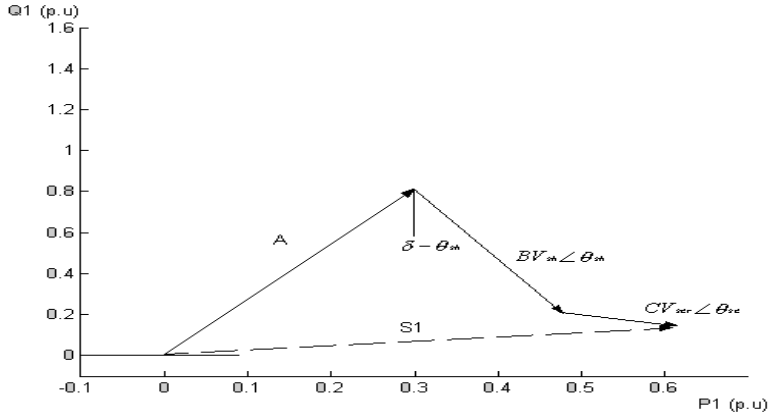

Fig. (6): Graphical representation of S_1 as a function of UPFC control variables

As θ_{ser} and (or) V_{ser} are changed to regulate power flow, θ_{sh} is also changed to ensure that $P_{ser} + P_{sh} = 0$. Thus, the tip of vector S_1 traces a closed path in the complex power plane of Fig. (6). This closed path is the power diagram of the tie line when the UPFC is in service. To identify the power diagram corresponding to (20), it can be decomposed to real and reactive powers as (22) and (23) respectively.

$$P_1 = a - c\sin(\delta - \theta_{ser}) \quad \text{Or} \quad P_1 - a = -c\sin(\delta - \theta_{ser}) \tag{23}$$

$$Q_1 = b + c\cos(\delta - \theta_{ser}) \quad \text{Or} \quad Q_1 - b = c\cos(\delta - \theta_{ser}) \tag{24}$$

Squaring equations (23) and (24) then adding them, results in equation (25)

$$(P_1 - a)^2 + (Q_1 - b)^2 = c^2 \tag{25}$$

Where:

$$a = \frac{X_{sh}V_1V_2}{X_t^2}\sin(\delta) + \frac{X_2V_1V_{sh}}{X_t^2}\sin(\delta - \theta_{sh})$$

$$b = \frac{(X_{sh} + X_2)V_1^2}{X_t^2} - \frac{X_{sh}V_1V_2}{X_t^2}\cos(\delta) - \frac{X_2V_1V_{sh}}{X_t^2}\cos(\delta - \theta_{sh})$$

$$c = \frac{X_{sh}V_{ser}V_1}{X_t^2}$$

If a and b are assumed as constant values, then (25) can represents a circle in the complex power plane. However, in general a and b in (25) can not be assumed as fixed values, since it is function of θ_{sh} and V_{sh}, which in turn are varied as a results of changing θ_{ser} and/or V_{ser}. Thus for different values of θ_{ser}, there are some different values for θ_{sh} as shown in Fig. (7). Fig. (8) shows the variation of the center (a,b) of the closed path due to the change of the series voltage source angle (θ_{ser}). Therefore (25) identifies a closed path, with constant radius c and centers on arc ef as shown in Fig. (9), which illustrates the tie line complex power region for different values of θ_{ser} and V_{ser}.

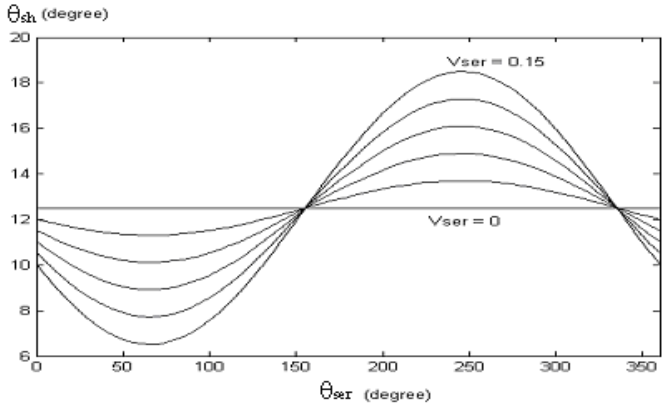

Fig. (7): Variation of (θ_{sh}) versus (θ_{ser}) at different values of the magnitude of series voltage and $\delta = 25^\circ$.

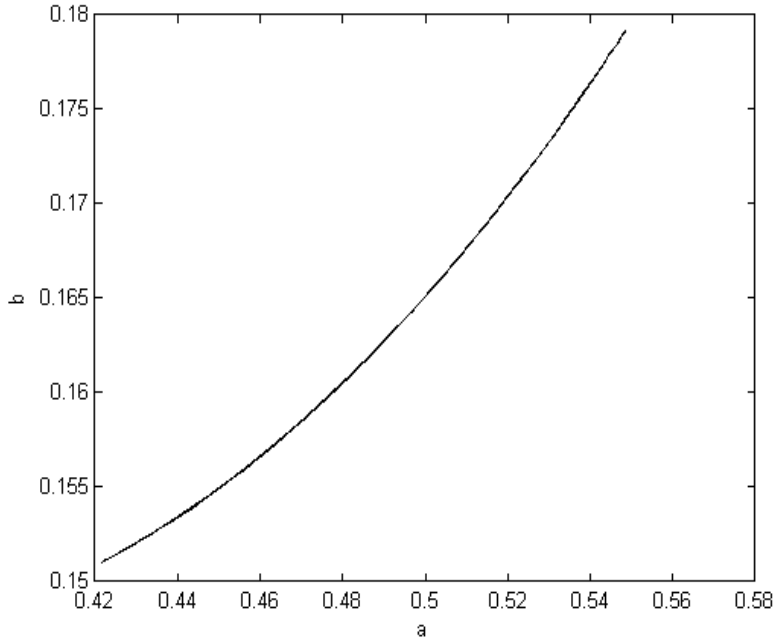

Fig. (8): variation of the center of the closed path (a,b) at different values of θ_{ser}

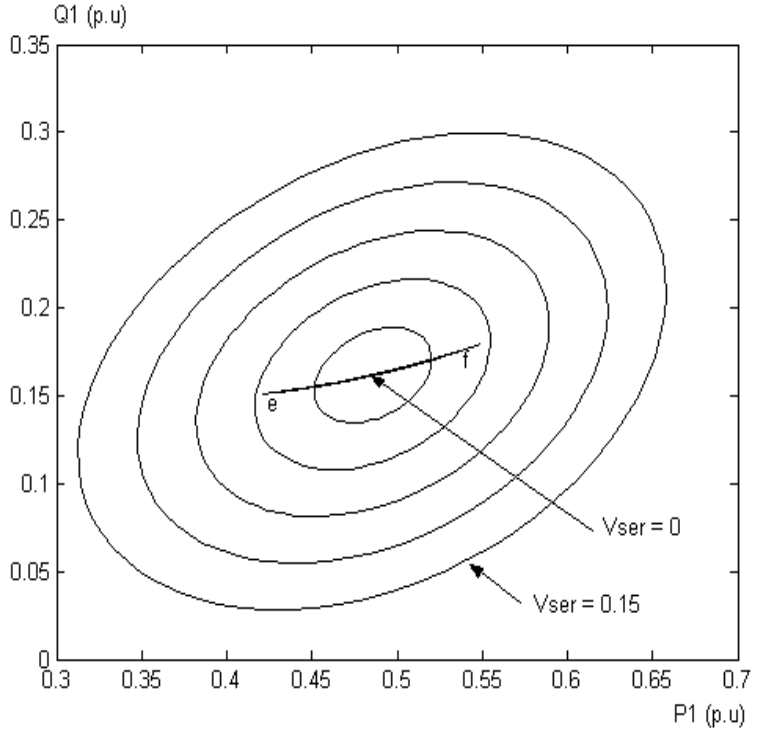

Fig. (9): The tie line complex power region at sending-end

3.2 Power Flow Characteristics at Receiving-End

The power flow characteristics at receiving-end with UPFC connected, can be visualized by rearranged equations (12) and (3) to be in the form of equations (26) and (27)

$$P_2 = a + c\sin\theta_{ser} \quad \text{or} \quad P_2 - a = c\sin\theta_{ser} \tag{26}$$

$$Q_2 = b - c\cos\theta_{ser} \quad \text{or} \quad Q_2 - b = -c\cos\theta_{ser} \tag{27}$$

Squaring equations (26) and (27) then adding them, results in equation (28)

$$(P_2 - a)^2 + (Q_2 - b)^2 = c^2 \tag{28}$$

Where:

$$a = \frac{X_{sh}V_1V_2}{X_t^2}\sin\delta + \frac{X_1V_2V_{sh}}{X_t^2}\sin\theta_{sh}$$

$$b = \frac{(X_{sh}+X_1)V_2^2}{X_t^2} - \frac{X_{sh}V_1V_2}{X_t^2}\cos\delta - \frac{X_1V_2V_{sh}}{X_t^2}\cos\theta_{sh} \quad c = \frac{(X_{sh}+X_1)V_2V_{ser}}{X_t^2}$$

Noting that $\delta = \delta_1$ and $\delta_2 = 0^\circ$ i.e. receiving-end is taken as reference.

Also the Q-P characteristics at the receiving-end appears as an ellipse where the radius c is constant but the center (a,b) is varied with the variation of θ_{sh} that varied according to the variation of θ_{ser} to achieve the constraint of $P_{ser} + P_{sh} = 0$. Figure (10) shows the Q-P characteristics at receiving-end at power angle $\delta = 25^\circ$ for different values of θ_{ser} from 0° to 360° and V_{ser} from 0 to 0.15 p.u.

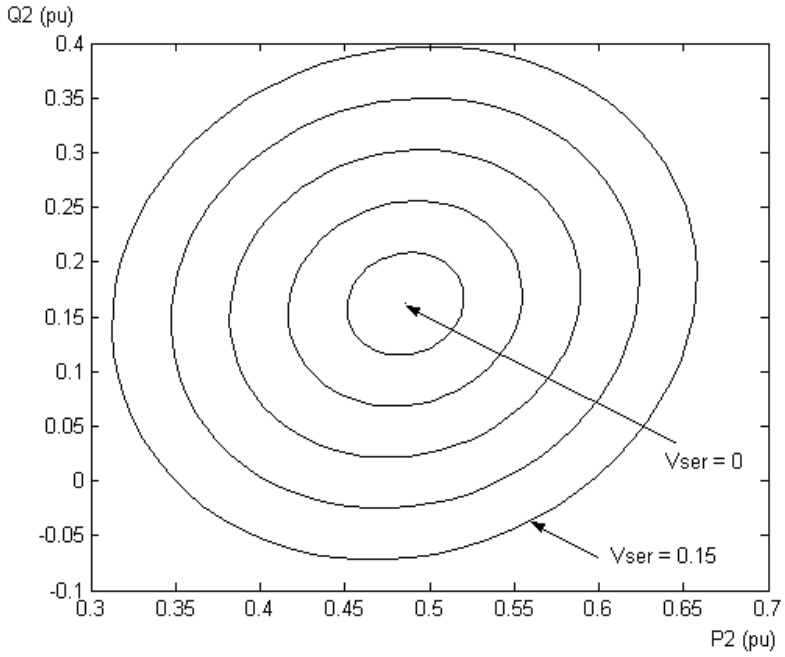

Fig. (10): The tie line complex power region at receiving-end

4. EFFECT OF THE SHUNT VOLTAGE SOURCE MAGNITUDE V_{SH} ON THE POWER FLOW CHARACTERISTICS

Figure (11) shows the Q-P characteristics at sending-end for different values of V_{sh} (0.9-1.1). This figure emphasize that when V_{sh} is larger than the system voltage, the UPFC injects reactive power into the system and vice versa. Also the Q-P curves at different values of V_{sh} are parallel and this emphasize that the injected shunt reactive power of UPFC are independent on the series power.

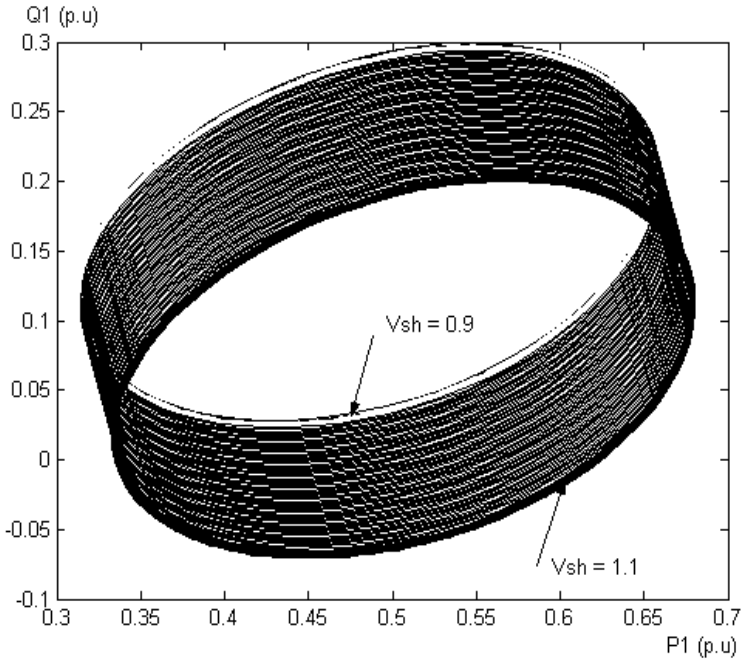

Fig. (11): The tie line complex power region at different values of V_{sh} (0.9-1.1) p.u., V_{ser} = 0.15 p.u., and $\delta = 25^{\circ}$

5. EFFECT OF SYSTEM POWER ANGLE ON POWER FLOW CHARACTERISTICS

The system power angle δ is another system parameter that can have the significant effect on tie line power transfer when the UPFC is in service. Fig. (1-18) depicts the complex power region that can be controlled by changing θ_{ser} from 0° to 360° for two different values of power angle δ.

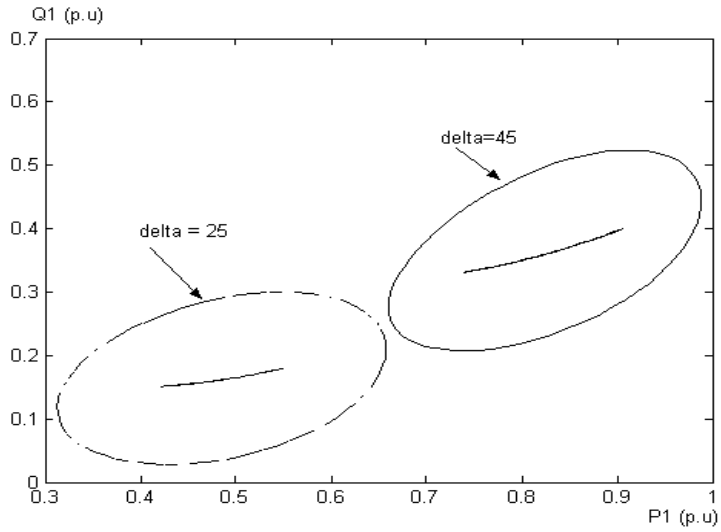

Fig. (12): Sending-end complex power for $\delta = 25^{\circ}$ and $\delta = 45^{\circ}$.

6. CONCLUSIONS

This paper identifies the effect of the UPFC control variables ($V_{ser}, \theta_{ser}, V_{sh}$, and θ_{sh}) on the line power transfer by using a form of vector presentation in complex power plane. The results show that:

- The amplitude V_{ser} and phase angle of series injected voltage θ_{ser} have the most effect of real power transfer if the power angle between two systems is small.
- For the large power angle, in addition to V_{ser} and θ_{ser}, the voltage amplitude of the parallel voltage V_{sh} can be used for the real power control. However, V_{sh} can control the line reactive power for the small power angle.
- The phase angle of parallel voltage θ_{sh} is set to regulate the DC link capacitor voltage V_{dc}.
- The results assure the independency of both series and shunt compensation of the UPFC.

REFERENCES

1. L. Gyugyi, "A Unified Power Flow Control Concept for Flexible AC Transmission Systems," IEE Proceeding, Vol.139, No.4, July 1992.
2. L. Gyugyi, T.R. Rietman, C. D. Schauder, D. R. Torgerson, S. L. Williams, and A. Edris, "The Unified Power Flow Controller: A New Approach to Power Transmission Control," IEEE Transactions on Power Delivery, Vol.10, No.2 pp. 1085-1092, April 1995.
3. N. G. Hingorani, L. Gyugyi, "Understanding FACTS, Concepts and Technology of Flexible AC Transmission Systems," IEEE Press, 2000.

4. L. Gyugyi, "Dynamic Compensation of AC Transmission Lines by Solid-State Synchronous Voltage Sources", IEEE/PES Summer Power Meeting, No. 93, Canada, July 1993.
5. S.A. Nabavi-Niaki, M.R. Iravani, "Investigation of Static-shifter Behavior under Steady-State Conditions", ICEE-94, pp. 126-134.
6. S.A. Nabavi-Niaki, "Visualization of UPFC Control Parameters Effects on the Tie-Line Power Flow", Proceeding of LESCOPE 2002, Nova Scotia, Canada, May 2002, pp. 103-107.
7. S.A. Nabavi-Niaki, M. R. Iravani, "Visualization and Investigation of Unified Power Flow Controller (UPFC) Non-Linearity in Power Flow", Power Engineering Society General Meeting, 2003, IEEE, Vol.2 pp. 812-817, July 2003.

نظرة على تأثير منظم مسارات القدرة الموحدة على منحنيات مسارات القدرة

يهدف البحث إلي دراسة وإلقاء نظرة على تأثير منظم مسارات القدرة الموحدة على منحنيات مسارات القدرة من خلال إدماج المنظم في نظام مكون من باسباران. هذا وقد تم تمثيل منظم مسارات القدرة الموحدة بمصدري جهد مثاليين يتصل بكلٍ منهما ممانعة على التوالي. والنموذج المقدم يلقي الضوء على العلاقة الغير خطية بين منظم مسارات القدرة الموحدة ومشكلة مسارات القدرة أنظمة القوى الكهربية. سوف يتم تمثيل المتغيرات المختلفة لمنظم مسارات القدرة الموحدة, والتى هي أصلاً غير خطية, كمتجة مركب وذلك لإلقاء الضوء ودراسة تأثير مختلف متغيرات التحكم للمنظم على سريان القدرة على الخط. وهذا يساعد في التعريف بتأثيرات كل متغير من متغيرات المنظم على التحكم في القدرة الكهربية المنقولة.